J. Fluid Mech. (1974), *vol.* 66, *part* 4, *pp.* 767–789
Printed in Great Britain

Separation and the Taylor-column problem for a hemisphere

By J. D. A. WALKER
School of Mechanical Engineering, Purdue University, West Lafayette, Indiana 47907
AND K. STEWARTSON
Department of Mathematics, University College, London

(Received 19 October 1973)

A layer of viscous incompressible fluid is confined between two horizontal plates which rotate rapidly in their own plane with a constant angular velocity. A hemisphere has its plane face joined to the lower plate and when a uniform flow is forced past such an obstacle, a Taylor column bounded by thin detached vertical shear layers forms. The linear theory for this problem, wherein the Rossby number ϵ is set equal to zero on the assumption that the flow is slow, is examined in detail. The nonlinear modifications of the shear layers are then investigated for the case when $\epsilon \sim E^{\frac{1}{3}}$, where E is the Ekman number. In particular, it is shown that provided that the Rossby number is large enough separation occurs in the free shear layers. The extension of the theory to flow past arbitrary spheroids is indicated.

1. Introduction

When a body translates through a contained rapidly rotating fluid the formation of a Taylor column bounded by thin detached shear layers is well documented. The phenomenon was first observed by Taylor (1923), who towed a short upright circular cylinder across the horizontal bottom of a rotating tank. His experiments have provoked numerous other investigations in which either various obstacles have been made to translate through the fluid or alternatively a flow has been forced past a stationary obstacle. In either situation the net effect is essentially the same.

When the speed U of the basic flow is very slow a slug of stagnant fluid is observed inside the cylinder $\mathscr{C}$ which circumscribes the obstacle and has generators parallel to the rotation vector. A set of thin detached vertical shear layers at $\mathscr{C}$ form the perimeter of the Taylor column. Outside $\mathscr{C}$ the fluid appears to move in a two-dimensional manner almost as if past a solid circular cylinder, the difference being that, no matter how small U is, there is always an observable asymmetry in the flow about the downstream radius. This may be readily seen, for example, by a careful inspection of a photograph by Baker (see Greenspan 1968, p. 3, plate 2(*b*)). As U is increased eventually a separated eddy appears behind the column and to the left (facing upstream) when the rotation is counterclockwise.

A further increase in U leads to a progressive deterioration of the situation as the convective terms in the equations of motion and three-dimensional effects assume an increasing importance. In an investigation by Hide, Ibbetson & Lighthill (1968), in which a flow transverse to the rotation axis was forced past a sphere, the axis of the Taylor column was observed to trail in the downstream direction and make a small angle $\psi = \tan^{-1}\{KU/2\Omega a\}$ with the rotation vector. Here Ω is the steady rotation rate, a is the radius of the sphere and K is a constant. The experiments of Hide and Ibbetson indicated the $K = 1{\cdot}54 \pm 0{\cdot}04$ while Lighthill predicted on a theoretical basis that $K = 1{\cdot}5$. An additional feature observed by Hide & Ibbetson (1966) in their study of the flow past a stubby circular cylinder is that the column recedes eventually from the cylinder $\mathscr{C}$ to the rear portion of the obstacle. The appearance of this 'partial' Taylor column is accompanied by a strong cross-flow over the front portion of the obstacle. Hide & Ibbetson (1966) also noted that the flow in the vicinity of the Taylor column was not completely stagnant and observed a feeble secondary flow there which they attributed to viscous effects. Obviously the flow at this stage is becoming rather complex and no attempt will be made here to describe these latter situations theoretically.

For motion that is very slow in the sense that the convective terms in the equations of motion may be neglected, the two-dimensional nature of the flow may be explained by the Taylor–Proudman theorem. However, when the flow field is unbounded in all directions, the solution of the steady inviscid equations is indeterminate (Taylor 1922). Grace (1926) considered the motion of a sphere transverse to the rotation axis in an unbounded fluid and attempted to solve the unsteady inviscid equations in the limit $\Omega t \to \infty$. His solution was completed, for the more general case of an ellipsoid, by Stewartson (1953), who showed that the flow became steady everywhere as $\Omega t \to \infty$ except in the immediate vicinity of $\mathscr{C}$. The main features of this solution were an asymmetric flow exterior to $\mathscr{C}$ with a flux across $\mathscr{C}$. At $\mathscr{C}$ the fluid particles change direction abruptly and inside $\mathscr{C}$ the particle paths lie on arcs of circles on spheres inscribed in $\mathscr{C}$. The difficulty with reconciling this solution with experiment is that physically the fluid is always bounded in the axial direction by two plates or perhaps a free surface instead of the upper plate. When this happens in other problems, theory and experiment may be reconciled by taking the axial extent of the fluid to be very large. In this case, because of the cylindrical character of the flow, this is not possible and here the presence of boundaries of the fluid in the axial direction, where the axial velocity is zero, is vital. This was pointed out by Stewartson (1967), who considered the unsteady inviscid motion of a sphere transverse to the rotation axis in a rotating fluid bounded by two horizontal plates a distance d apart. The ultimate steady motion was shown to be stagnant above the sphere while outside $\mathscr{C}$ the fluid moves around $\mathscr{C}$ as if past a solid cylinder. Since the convective terms were ignored in this approach, the analysis is subject to the restriction $U/\Omega a \ll 1$ and formally corresponds to the limit sequence $\nu \to 0$, $t \to \infty$, where ν is the coefficient of kinematic viscosity.

Another point of interest in this connexion is the ultimate steady force exerted on the sphere. Stewartson (1967) showed that while there is no drag force on the

sphere there is a sideways or deflecting force equal to $\frac{8}{3}\pi\rho a^3 U\Omega$. If the density of the sphere and fluid are equal this force just balances the Coriolis force. A series of experiments carried out at the Meteorological Office in Bracknell, England, confirms the general magnitude of the predicted deflecting force (R. Hide, private communication). In more general terms, the results concerning the forces on bodies in rotating fluids may be briefly summarized as follows. Suppose that L is the linear dimension of the body and h and d are the axial extent of the body and fluid, respectively. It is found that, when the ratio h/d is large with respect to $U/\Omega L$, the drag force on the body is very small but the deflecting force (perpendicular to the motion) is appreciable. In the case of an upright cylindrical body the value of the deflecting force is approximately equal to (for very slow motion) or less than $2\rho\Omega UA$ per unit height, where A is the cross-sectional area of the cylinder. This value may be predicted from linear inviscid theory. Conversely, as h/d becomes small with respect to $U/\Omega L$ the situation reverses; the drag becomes the dominant force and the deflecting force becomes small.

A different limit approach to the Taylor-column problem was taken by Jacobs (1964), who considered the case of flow, transverse to the rotation axis, past a symmetrical obstacle located on the lower of two rapidly rotating horizontal plates. Let z measure distance above the lower plate and r measure distance from the symmetry axis of the obstacle. Suppose that $z = b(r)$ is the equation of the obstacle and $b'(a)$ and $b''(a)$ are the slope and curvature at the rim of the obstacle at $r = a$. Then Jacobs' (1964) analysis is concerned with cases where $b'(a)$ and $b''(a)$ are $O(1)$. The flow was analysed on the basis of linear theory wherein the basic flow is assumed so slow that the inertial terms in the equations of motion are neglected. It was shown that in this situation the geostrophic motion consistent with the Ekman layers is a stagnant one above the obstacle while elsewhere the geostrophic solution is an irrotational potential flow which to leading order passes symmetrically by the Taylor column as if it were a solid cylinder. We note here that this procedure corresponds to the limit sequence $t \to \infty$, $\nu \to 0$ and that the non-uniqueness in the inviscid steady equations has been removed by Ekman boundary layers on the horizontal surfaces and on the obstacle. Evidently both limit sequences are complementary and as far as the determination of the inviscid flow is concerned, neither limit sequence is preferred as both lead to the same solution. A discussion of the significance of the different limit sequences is given in Hide *et al.* (1968).

Jacobs (1964) then went on to analyse the thin detached $E^{\frac{1}{4}}$ layers which partially define the column and which provide the smooth transition from the exterior potential flow to the stagnant interior. Since separation is a nonlinear phenomenon, it is not surprising that Jacobs (1964) did not predict the separated eddy that had been observed behind the column by Taylor (1923) and by many others. This, of course, does not imply that this is always the case and the photograph by Baker in Greenspan (1968, p. 3) provides an experimental example of an apparently unseparated slow flow. In the present paper, the flow past symmetrical obstacles which have an infinite slope at the rim is considered and of most concern is the problem of flow past a hemispherical bump.

Let us now fix the problem mathematically. Suppose that a layer of viscous

incompressible fluid is contained between two rigid horizontal plates of infinite extent at $z^* = 0$ and $z^* = d$. A symmetrical obstacle has its base joined to the lower plate and the base radius is ad. The whole system rotates with a constant angular velocity Ω about an axis perpendicular to the plates and a flow, transverse to the rotation axis and having speed U, is forced past the bump. In practice this might be accomplished by the source–sink arrangement of Hide *et al.* (1968) or, in order to achieve the same net effect, by towing the obstacle across the tank bottom as in Hide & Ibbetson (1966). The equations governing the steady motion and written in a frame that rotates uniformly with the plates are

$$\left.\begin{aligned} \epsilon(\mathbf{q}.\nabla)\,\mathbf{q} + 2(\hat{\mathbf{z}}\times\mathbf{q}) &= -\nabla p - E\nabla\times(\nabla\times\mathbf{q}),\\ \nabla.\mathbf{q} &= 0. \end{aligned}\right\} \tag{1}$$

Here $\mathbf{q}$ is the velocity vector and $\hat{\mathbf{z}}$ a unit vector perpendicular to the plates. In these equations the physical quantities have been made dimensionless by

$$\mathbf{r}^* = d\mathbf{r}, \quad \mathbf{q}^* = U\mathbf{q}, \quad p^* = (\rho\Omega U d)\,p,$$

where a star indicates a dimensional quantity and ρ and p are the constant density and reduced pressure respectively. The two dimensionless numbers governing the motion are the Rossby number ϵ and the Ekman number E, defined as

$$\epsilon = U/\Omega d, \quad E = \nu/\Omega d^2.$$

The linear theory ($\epsilon = 0$) of the flow past a hemispherical bump is next examined in detail with two aims in mind. First, Jacobs' (1964) analysis applies only to lenticular bodies, that is bodies for which $z \sim (a-r)$ near the rim at $r = a$, and we extend it to those for which $z \sim (a-r)^n$ near the rim, where $0 < n < 1$. Here a is the dimensionless radius of the bump. For the hemisphere $n = \frac{1}{2}$ and for the problem studied experimentally by Hide & Ibbetson (1966), namely the right circular cylindrical bump, $n = 0$. The perturbation analysis of the shear layers for this problem is complex and considerable attention is devoted to the development of a logical analysis of this in § 2. The second and central aim is to form the foundation for a consistent treatment of the nonlinear theory ($\epsilon \sim E^{\frac{1}{2}}$) in § 3. In particular, the principal result required for the nonlinear analysis is derived in § 2.3, where it is shown that to leading order the flow in the external $E^{\frac{1}{4}}$ layer of the Taylor column is identical to that in the $E^{\frac{1}{4}}$ layer for flow past a solid circular cylinder.

The assumption is made at the outset that the flow takes place in a rapidly rotating frame in the sense that the Ekman number $E \ll 1$. The velocity components and pressure in the vertical shear layers will subsequently be expanded in powers of the Ekman number and on occasion in the formal expansion it is necessary to introduce small exponents of E. We remark here that in the experimental context it is unrealistic to make an order-of-magnitude distinction between say $E^{\frac{1}{28}}$ and $E^{\frac{1}{14}}$. However, it is not our purpose here to model closely the experimental situation but rather to attempt to explain on the basis of boundary-layer theory some of the observed features of the flow. In particular two things are of interest. First, although the leading-order geostrophic flow around the column is a symmetrical potential flow identical to the ideal flow past a solid

circular cylinder, a weak asymmetrical geostrophic flow is generated for $r > a$ by an asymmetrical flow in the vertical shear layers. This feature of the flow is discussed in § 2.9 on the basis of linear theory. The second and main point of interest is that separation occurs in a free shear layer. This is a rather novel phenomenon in that separation occurs at a fluid–fluid interface and it is of interest to understand how this arises. The simplest obstacle to consider for this purpose is the hemisphere because the various shear layers that form the perimeter of the Taylor column all have a different thickness. This does mean, however, that the expansions proceed in powers of $E^{\frac{1}{2}\frac{1}{8}}$, which severely limits the quantitative value of the theory. Nevertheless, from a qualitative standpoint, the leading terms we consider do fix the character of the motion and show how separation can occur. In particular, it is shown in § 3 that when the Rossby number has a quite small value $[O(E^{\frac{1}{2}})]$ separation occurs in the $E^{\frac{1}{4}}$ layer. In § 4 the extension of the theory to flow past arbitrary spheroids is discussed.

2. Linear theory

2.1. *The geostrophic flow*

Throughout the majority of the fluid, the flow is geostrophic, arising from a balance between the pressure gradient and the Coriolis force in (1). The Taylor–Proudman theorem demands that this flow be independent of z. This solution in general fails to satisfy the no-slip condition at solid boundaries, and on all horizontal boundaries and on the obstacle itself the flow is brought to relative rest by viscous forces in thin Ekman layers in a length scale $O(E^{\frac{1}{2}})$.

Let (r, θ, z) be cylindrical co-ordinates centred on the symmetry axis and with origin at the base of the obstacle with corresponding velocity components (u, v, w) and $\theta = 0$ being the downstream radius. The linear solution for the flow in the Ekman layers on horizontal surfaces is well known. In particular, the Ekman layers control the geostrophic flow through the Ekman suction conditions. For horizontal boundaries these conditions are

$$W_G = \pm \tfrac{1}{2} E^{\frac{1}{2}} \zeta_G \quad \text{at} \quad z = \tfrac{1}{2} \mp \tfrac{1}{2}, \tag{2}$$

where W_G and ζ_G are the vertical velocity and vorticity respectively in the geostrophic interior. Because the interior flow is independent of z, this implies that

$$W_G = \zeta_G = 0$$

in all regions where one horizontal surface is directly above another. In the case of the hemisphere, the Ekman suction condition can be shown to take the more complicated form

$$W_G + \frac{rU_G}{(a^2-r^2)^{\frac{1}{2}}} = \frac{E^{\frac{1}{2}}}{2r}\left[\frac{1}{(1-r^2/a^2)^{\frac{3}{4}}}\frac{\partial}{\partial\theta}\left\{V_G + \frac{r}{a}W_G - \frac{U_G(a^2-r^2)^{\frac{1}{2}}}{a}\right\}\right.$$
$$\left. + \left(\frac{\partial}{\partial r} - \frac{r}{(a^2-r^2)^{\frac{1}{2}}}\frac{\partial}{\partial z}\right)\left\{\frac{r}{(1-r^2/a^2)^{\frac{1}{4}}}\left(V_G - W_G\frac{r}{a} + \frac{U_G(a^2-r^2)^{\frac{1}{2}}}{a}\right)\right\}\right] \tag{3}$$

on the sphere $z = (a^2-r^2)^{\frac{1}{2}}$, where a is the dimensionless radius of the sphere. It can be easily shown using an argument similar to that of Jacobs (1964) for a

lenticular body that the only geostrophic motion compatible with the condition (3) and the Ekman conditon (2) at $z = 1$ is the stagnant solution.

The discontinuity in the geostrophic flow at the cylinder $r = a$ is adjusted by means of detached vertical shear layers which form the boundary of the Taylor column. Since an $O(1)$ adjustment in the swirl velocity is required and since the radial pressure gradient and Coriolis force balance in the shear layers, the pressure adjustment is of lower order across the shear layers. Thus to leading order the geostrophic pressure must be continuous at $r = a$ and this leads to the result that to leading order

$$\left.\begin{aligned} U_G = V_G = W_G = 0 \quad \text{for} \quad r < a, \\ U_G = \cos\theta\{1-a^2/r^2\}, \quad V_G = -\sin\theta\{1+a^2/r^2\}, \quad W_G = 0 \quad \text{for} \quad r > a. \end{aligned}\right\} \tag{4}$$

Here the possibility of a constant relative circulation $O(1)$ for $r > a$ has been excluded since this would result in a radial flux $O(E^{\frac{1}{2}})$ in the Ekman layers on the horizontal plates. This flux would be independent of θ and its direction would be the same on both the top and bottom plate. Across any cylindrical control surface enveloping the Taylor column and having generators perpendicular to the plates there would then be a net influx or efflux through the Ekman layers depending on the sense of the circulation. Since there is no possible geostrophic flow to balance this, a steady circulation is not possible unless there are sources or sinks within the fluid.

2.2. *The shear layers*

The basic shear-layer structure for a spherical body has been given in detail by Stewartson (1966) in connexion with his study of the flow between two rotating concentric spheres that have slightly different rotation rates. The structure consists of an external $E^{\frac{1}{4}}$ layer at $r = a+$ and an internal $E^{\frac{2}{7}}$ layer at $r = a-$ above the sphere. Sandwiched between the $E^{\frac{2}{7}}$ and $E^{\frac{1}{4}}$ layers there is an inner layer of thickness $O(E^{\frac{1}{3}})$. It was shown by Stewartson (1966) that the $E^{\frac{1}{3}}$ layer could not adjust a discontinuity in either the swirl velocity or tangential stress and both of these quantities must be continuous across the $E^{\frac{1}{3}}$ layer. The role of the $E^{\frac{1}{3}}$ layer is to remove discontinuities in higher-order derivatives of v with respect to r. Physically the $E^{\frac{1}{3}}$ layer in many problems recirculates mass to leading order (Moore & Saffman 1969*a*). An additional complication arises with the Ekman layers. On all horizontal surfaces and on the major portion of the hemisphere, these layers have a thickness $O(E^{\frac{1}{2}})$. However near the equator and underneath the $E^{\frac{1}{3}}$ layer in a vertical length scale $O(E^{\frac{1}{5}})$ the Ekman layer thickens to have a width $O(E^{\frac{2}{5}})$. The structure is shown schematically in figure 1.

Within the $E^{\frac{1}{4}}$ layer at $r = a+$, the leading terms in the expansions for the velocity components and pressure are written as

$$\left.\begin{aligned} u_{\frac{1}{4}} = (2^{\frac{1}{2}}a)^{-1}E^{\frac{1}{4}}u_0(\xi,\theta)+\ldots, \quad v_{\frac{1}{4}} = v_0(\xi,\theta)+\ldots, \\ w_{\frac{1}{4}} = 2^{\frac{1}{2}}E^{\frac{1}{4}}w_0(\xi,\theta,z)+\ldots, \quad p_{\frac{1}{4}} = 2^{\frac{1}{2}}E^{\frac{1}{4}}p_0(\xi,\theta)+\ldots, \end{aligned}\right\} \tag{5}$$

where $\xi = 2^{\frac{1}{2}}(r-a)\,E^{-\frac{1}{4}}$ is the scaled radial variable in the $E^{\frac{1}{4}}$ layer. The Ekman compatibility conditions are, for $\xi > 0$,

$$w_0 = \pm\tfrac{1}{2}\,\partial v_0/\partial\xi + O(E^{\frac{1}{4}}) \quad \text{at} \quad z = \tfrac{1}{2}\mp\tfrac{1}{2}, \tag{6}$$

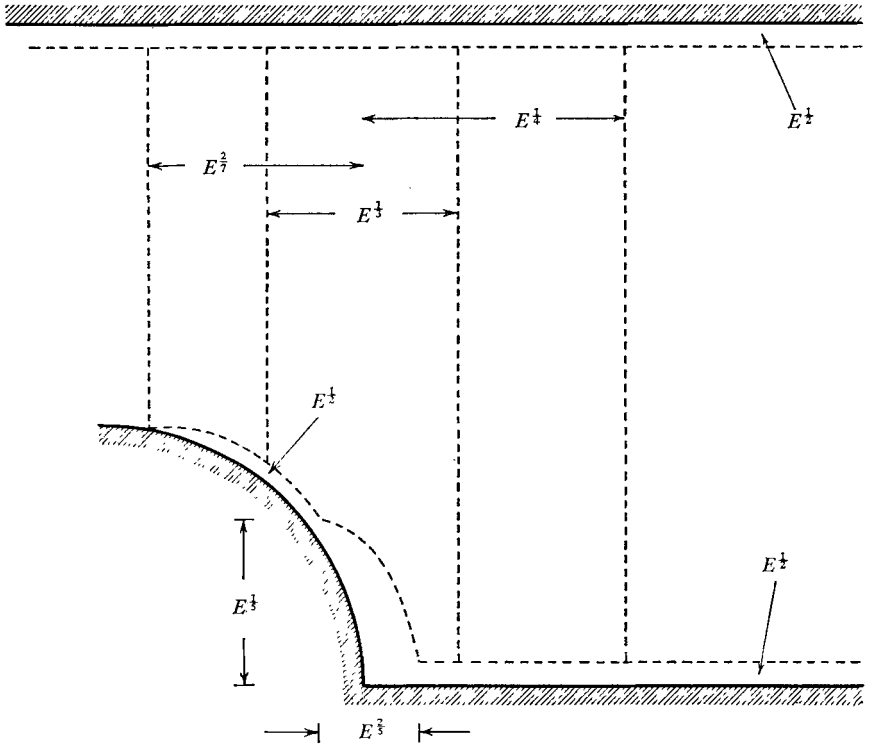

FIGURE 1. Shear-layer structure for a hemisphere (not to scale).

and u_0 and v_0 can be shown to satisfy the equations

$$\frac{\partial^3 v_0}{\partial \xi^3} - \frac{\partial v_0}{\partial \xi} = 0, \quad \frac{\partial u_0}{\partial \xi} = -\frac{\partial v_0}{\partial \theta},$$

with an error $O(E^{\frac{1}{4}})$. The solution which matches smoothly into the geostrophic flow is

$$v_0 = C(\theta)\, e^{-\xi} - 2\sin\theta, \quad u_0 = C'(\theta)\, e^{-\xi} + 2\xi\cos\theta + D(\theta),$$

where C and D are as yet undetermined functions of θ.

In the $E^{\frac{2}{7}}$ layer, the velocity components and pressure are written to leading order as

$$\left.\begin{aligned} u_{\frac{2}{7}} &= a^{-1}(2/a)^{\frac{2}{7}} E^{\alpha+\frac{2}{7}} \bar{u}_0(s,\theta) + \ldots, \quad v_{\frac{2}{7}} = (2/a)^{\frac{1}{7}} E^{\alpha} \bar{v}_0(s,\theta) + \ldots, \\ w_{\frac{2}{7}} &= (\tfrac{1}{2}a)^{\frac{2}{7}} E^{\alpha+\frac{1}{7}} \bar{w}_0(s,\theta,z) + \ldots, \quad p_{\frac{2}{7}} = (2/a)^{\frac{2}{7}} E^{\alpha+\frac{2}{7}} \bar{p}_0(s,\theta) + , \end{aligned}\right\} \tag{7}$$

where $s = (\frac{1}{2}a)^{\frac{1}{7}}(a-r)\, E^{-\frac{2}{7}}$ is the scaled radial variable in the $E^{\frac{2}{7}}$ layer. The functions $\bar{u}_0$, $\bar{v}_0$, $\bar{w}_0$ and $\bar{p}_0$ are $O(1)$ functions of s and θ, and the scaling index α is as yet undetermined. Eliminating the pressure in the momentum equations, we obtain

$$\partial^3 \bar{v}_0 / \partial s^3 = 2\, \partial \bar{w}_0 / \partial z. \tag{8}$$

The Ekman conditions for $s > 0$ become

$$\bar{w}_0 = 0 \quad \text{at} \quad z = 1,$$

with an error $O(E^{\frac{1}{14}})$. The equation of the hemisphere is $z \sim s^{\frac{1}{2}}E^{\frac{1}{7}}$ and

$$\bar{w}_0 = -\frac{\bar{u}_0}{as^{\frac{1}{2}}} - \frac{1}{2}\frac{\partial}{\partial s}\left(\frac{\bar{v}_0}{s^{\frac{1}{4}}}\right) + O(E^{\frac{1}{7}}) \quad \text{at} \quad z = 0,$$

where the boundary-layer approximation to the sphere has been made. Integration of (8) from $z = 0$ to $z = 1$ and application of the Ekman conditions gives

$$\frac{\partial^3 \bar{v}_0}{\partial s^3} - \frac{\partial}{\partial s}\left(\frac{\bar{v}_0}{s^{\frac{1}{4}}}\right) - \frac{2\bar{u}_0}{as^{\frac{1}{2}}} = 0,$$

with

$$\partial \bar{u}_0/\partial s = \partial \bar{v}_0/\partial \theta.$$

We may now eliminate the possibility of a non-trivial axisymmetric solution of this system. Since a constant relative circulation in either geostrophic region is not possible, the form of an axisymmetric solution in the $E^{\frac{1}{4}}$ and $E^{\frac{2}{7}}$ layers must be

$$v_0 = Ae^{-\xi}, \quad \bar{v}_0 = Bs^{\frac{1}{2}}K_{\frac{4}{7}}(\tfrac{8}{7}s^{\frac{7}{8}}),$$

where $K_{\frac{4}{7}}$ is the Bessel function of imaginary argument. The only values of the constants A and B consistent with continuity of v and $\partial v/\partial r$ at $\xi = s = 0$ are $A = B = 0$.

The functions $\bar{u}_0$ and $\bar{v}_0$ are then assumed to be

$$\bar{u}_0 = \mathrm{Re}\,(f(s)\,e^{i\theta}), \quad \bar{v}_0 = \mathrm{Re}\,(-if'(s)\,e^{i\theta}),$$

where $f(s)$ satisfies

$$f^{\mathrm{iv}} - (f'/s^{\frac{1}{4}})' - 2if/as^{\frac{1}{2}} = 0, \tag{9}$$

with $f \to 0$ as $s \to \infty$. The primes denote differentiation with respect to s. The solutions of (9) behave like

$$f \sim s^{-\frac{3}{16}}\exp\{\tfrac{8}{7}\gamma s^{\frac{7}{8}}\}$$

for large s, where γ satisfies the quartic

$$\gamma^4 - \gamma^2 - 2i/a = 0. \tag{10}$$

Hence for large s the solutions of (9) either increase or decrease exponentially. In the present context, acceptable solutions are given by $\gamma = \gamma_1, \gamma_2$, where γ_1 and γ_2 are the roots of (10) having negative real parts:

$$\gamma_1, \gamma_2 = -\{\tfrac{1}{2}[1 \pm (1 + 8i/a)^{\frac{1}{2}}]\}^{\frac{1}{2}}.$$

For small s, the differential equation shows that

$$f = a_0\{1 + \tfrac{32}{105}is^{\frac{7}{2}} + \ldots\} + a_1\{s + \tfrac{64}{231}s^{\frac{11}{4}} + \ldots\}$$
$$+ a_2\{s^2 + \tfrac{128}{1155}s^{\frac{15}{4}} + \ldots\} + a_3\{s^3 + \tfrac{192}{3135}s^{\frac{19}{4}} \ldots + \},$$

where a_0, a_1, a_2 and a_3 are arbitrary constants. The analytical solution of (9) is not known and it will subsequently be solved numerically. It is however clear at this stage that continuity of v and $\partial v/\partial r$ as ξ and s tend to zero will not yield sufficient conditions to effect a join with the $E^{\frac{1}{4}}$ layer and determine the solution. The extra needed condition comes from consideration of conservation of flux in the $E^{\frac{1}{3}}$ layer and is similar to an argument used by Moore & Saffman (1969*b*) in their study of the transverse motion of a thin disk in a rotating fluid.

2.3. *The flux condition*

In the Ekman layer under the external $E^{\frac{1}{4}}$ layer, to leading order, there is a radial flux of fluid per unit length of circumference in the $-r$ direction equal to

$$Q_{\frac{1}{4}}(\xi,\theta) = \tfrac{1}{2}E^{\frac{1}{4}}v_{\frac{1}{4}}(\xi,\theta).$$

Similarly, in the Ekman layer under the $E^{\frac{2}{7}}$ layer there is a flux per unit length of circumference whose direction is tangential to the sphere in the $+r$ direction and is to leading order

$$Q_{\frac{2}{7}}(s,\theta) = -\tfrac{1}{2}E^{\frac{3}{7}}(\tfrac{1}{2}a)^{\frac{2}{7}}v_{\frac{2}{7}}/s^{\frac{1}{4}}.$$

Thus there is a net flux $Q(\theta)$, per unit length of circumference, into the Ekman layer under the $E^{\frac{1}{3}}$ layer; $Q(\theta)$ consists of the sum of $Q_{\frac{1}{4}}$ evaluated at $\xi = 0+$ and $Q_{\frac{2}{7}}$ evaluated for $s \ll 1$. We note here that the contribution from $Q_{\frac{2}{7}}(s,\theta)$ is divergent as $s \to 0+$. Thus we require that $s \ll 1$ but $sE^{-\frac{1}{21}} \gg 1$; this is the region where the match with the solutions in the $E^{\frac{2}{7}}$ and $E^{\frac{1}{3}}$ layers takes place.

Consider now the $E^{\frac{1}{3}}$ layer. In this layer $v_{\frac{1}{3}}$ and $w_{\frac{1}{3}}$ are of the same order of magnitude and $u_{\frac{1}{3}}$ is $O(E^{\frac{1}{3}}v_{\frac{1}{3}})$. Let $\eta = (r-a)E^{-\frac{1}{3}}$ be the scaled radial variable in the $E^{\frac{1}{3}}$ layer; the Ekman conditions are then, to leading order,

$$w_{\frac{1}{3}} = -\tfrac{1}{2}E^{\frac{1}{6}}\frac{\partial v_{\frac{1}{3}}}{\partial \eta} \quad \text{at} \quad z = 1-, \quad \text{all } \eta, \quad w_{\frac{1}{3}} = \tfrac{1}{2}E^{\frac{1}{6}}\frac{\partial v_{\frac{1}{3}}}{\partial \eta} \quad \text{at} \quad z = 0+, \quad \eta > 0,$$

$$w_{\frac{1}{3}} = \tfrac{1}{2}E^{\frac{1}{12}}\left(\frac{a}{2}\right)^{\frac{1}{4}}\frac{\partial}{\partial \eta}\left\{\frac{v_{\frac{1}{3}}-w_{\frac{1}{3}}}{(-\eta)^{\frac{1}{4}}}\right\} \quad \text{at} \quad z = 2^{\frac{1}{2}}a^{\frac{1}{2}}(-\eta)^{\frac{1}{2}}E^{\frac{1}{6}}, \quad \eta < 0.$$

Hence to leading order $w_{\frac{1}{3}} = 0$ at $z = 0+$ and $1-$, where the boundary-layer approximation to the hemisphere has been used, and it appears that the $E^{\frac{1}{3}}$ layer cannot draw fluid from the Ekman layer to leading order. The possibility that the net flux can be closed by a swirl velocity in the $E^{\frac{2}{3}}$ layer can be eliminated since to preserve continuity such a velocity would necessarily be of higher order in E than that in the geostrophic flow. In fact, fluid passes into the $E^{\frac{1}{3}}$ layer through the equatorial boundary layer. This is an annular region having a lateral scale $O(E^{\frac{2}{3}})$ and a vertical scale $O(E^{\frac{1}{3}})$ and on the scale of the $E^{\frac{1}{3}}$ layer appears as a region of zero thickness. This singular type of behaviour is associated with the discontinuity in the bottom slope at the equator of the hemisphere. At the top plate there is no discontinuity and no net transfer of fluid into the $E^{\frac{1}{3}}$ layer takes place to leading order.

Consider now the $E^{\frac{1}{3}}$-layer equation

$$\partial^3 v_{\frac{1}{3}}/\partial\eta^3 = -2\,\partial w_{\frac{1}{3}}/\partial z,$$

and integrate this equation across the $E^{\frac{1}{3}}$ layer at constant z outside the equatorial boundary layer and Ekman layer on the top plate:

$$-2\frac{\partial}{\partial z}\int_{-\infty}^{\infty} w_{\frac{1}{3}}(\eta,\theta,z)\,d\eta = \left.\frac{\partial^2 v_{\frac{1}{3}}}{\partial\eta^2}\right|_{\eta=+\infty} - \left.\frac{\partial^2 v_{\frac{1}{3}}}{\partial\eta^2}\right|_{\eta=-\infty}$$

The variable η is related to ξ and s by

$$\xi = 2^{\frac{1}{2}}\eta E^{\frac{1}{12}}, \quad s = -\eta(\tfrac{1}{2}a)^{\frac{1}{7}}E^{\frac{1}{21}}$$

and since $v_{\frac{1}{3}}(\eta, \theta, z)$ as $\eta \to \pm\infty$ must match $v_{\frac{1}{4}}(\xi, \theta)$ as $\xi \to 0+$ and $v_{\frac{2}{7}}(s, \theta)$ for $s \ll 1$ respectively,

$$-2\frac{\partial}{\partial z}\int_{-\infty}^{\infty} w_{\frac{1}{3}}\, d\eta = 2E^{\frac{1}{6}}\frac{\partial^2 v_{\frac{1}{4}}}{\partial \xi^2}\bigg|_{\xi=0+} - \left(\frac{a}{2}\right)^{\frac{2}{7}} E^{\frac{2}{21}}\frac{\partial^2 v_{\frac{2}{7}}}{\partial s^2}\bigg|_{s\ll 1}.$$

At this stage it is uncertain which term is most important on the right side of this equation and so both are retained. We now integrate from $z = 0+$ (just above the equatorial boundary layer) to $z = 1-$ (just below the Ekman layer on the top plate) and since $w_{\frac{1}{3}}(\eta, \theta, 1-)$ vanishes for all η

$$\int_{-\infty}^{\infty} w_{\frac{1}{3}}(\eta, \theta, 0+)\, dr = E^{\frac{1}{2}}\frac{\partial^2 v_{\frac{1}{4}}}{\partial \xi^2}\bigg|_{\xi=0+} - \frac{1}{2}\left(\frac{a}{2}\right)^{\frac{2}{7}} E^{\frac{3}{7}}\frac{\partial^2 v_{\frac{2}{7}}}{\partial s^2}\bigg|_{s\ll 1},$$

which must equal the inflow $Q(\theta)$. Therefore, to leading order,

$$\frac{E^{\frac{3}{7}}}{2}\left(\frac{a}{2}\right)^{\frac{2}{7}} \lim_{s\to 0+}\left\{\frac{\partial^2 v_{\frac{2}{7}}}{\partial s^2} - \frac{v_{\frac{2}{7}}}{s^{\frac{1}{4}}}\right\} - E^{\frac{1}{2}} \lim_{\xi\to 0+}\left\{\frac{\partial^2 v_{\frac{1}{4}}}{\partial \xi^2} - \frac{v_{\frac{1}{4}}}{2}\right\} = 0. \tag{11}$$

This condition and continuity of swirl velocity

$$v_{\frac{2}{7}}(0, \theta) = v_{\frac{1}{4}}(0, \theta) \tag{12}$$

and tangential stress

$$\frac{\partial v_{\frac{2}{7}}}{\partial s}(0, \theta) = -2^{\frac{1}{2}}\left(\frac{2}{a}\right)^{\frac{1}{7}} E^{\frac{1}{28}}\frac{\partial v_{\frac{1}{4}}}{\partial \xi}(0, \theta) \tag{13}$$

across the $E^{\frac{1}{4}}$ layer are sufficient to determine the solution in the outer shear layers.

In order to determine α, the scaling index in the $E^{\frac{2}{7}}$ layer, we first suppose that $\alpha < \frac{1}{28}$. Conditions (13) and (11) lead to the following boundary conditions for f:

$$f''(0) = 0, \quad \lim_{s\to 0+}\{f''' - f'/s^{\frac{1}{4}}\} = 0. \tag{14}$$

Suppose that $f(s)$ is a non-trivial solution of (9) satisfying conditions (14) which vanishes at infinity. Equation (9) is multiplied by $f^*(s)$, where the star indicates the complex conjugate, and integrated from $s = 0$ to $s = \infty$. Two integrations by parts and application of conditions (14) lead to

$$\int_0^{\infty}\left\{|f''|^2 + \frac{|f'|^2}{s^{\frac{1}{4}}} - \frac{2i}{as^{\frac{1}{2}}}|f|^2\right\} ds = 0.$$

Here the fact that f^* vanishes at infinity if f does has been used and also the fact that f and f^* and their first derivatives are bounded at $s = 0$. Thus $f(s)$ is forced equal to zero.

Any choice $\alpha > \frac{1}{28}$ for the leading term leads to a contradiction regarding the function $C(\theta)$ in the external $E^{\frac{1}{4}}$ layer and therefore the index of the leading term in the $E^{\frac{2}{7}}$ layer is $\alpha = \frac{1}{28}$ with

$$f''(0) = 2^{\frac{3}{2}}, \quad \lim_{s\to 0}\{f''' - f'/s_{\frac{1}{4}}\} = 0. \tag{15}$$

In addition, $$u_0(0, \theta) = v_0(0, \theta) = 0,$$

so that $C(\theta) = 2\sin\theta$ and $D(\theta) = -2\cos\theta$ and to leading order the solution in the external $E^{\frac{1}{4}}$ layer is a symmetrical flow identical to that for flow past a solid circular cylinder in a rotating frame (Walker & Stewartson 1972). The solution for the leading-order flow in the $E^{\frac{2}{7}}$ layer was obtained numerically and the method of solution is described in the following section.

2.4. *Numerical solution*

The function $f(s)$ has an irregular behaviour near $s = 0$ in that f''' and all higher derivatives with respect to s are large there. The function may be regularized by setting $x = s^{\frac{1}{4}}$ but for large s this is not appropriate. Because of this (9) was solved numerically in two ranges. For s lying in the range $[0, 1]$ we set $x = s^{\frac{1}{4}}$ and defining auxiliary functions $p(x)$, $q(x)$ and $y(x)$, equation (9) becomes

$$\left.\begin{aligned} df/dx &= 4x^3p, \qquad dp/dx = 4x^3q, \\ dq/dx &= 4x^3y + 4x^2p, \quad dy/dx = 8ixf/a, \end{aligned}\right\} \tag{16}$$

with $$f(0) = a_0, \quad p(0) = a_1, \quad q(0) = 2^{\frac{3}{2}}, \quad y(0) = 0.$$

Here a_0 and a_1 are the unknown values of f and f' at $s = 0$.

For s lying in the range $[1, \infty)$, the derivatives in (9) were approximated by central differences, giving a set of difference equations

$$f_{n-2} + c_n f_{n-1} + \alpha_n f_n + b_n f_{n+1} + f_{n+2} = 0 \tag{17}$$

at grid points $s_n = 1 + nh$ for $n = 1, 2, 3, \ldots, n_0$, where $n_0 = (l - 1 - 2h)/h$. Here h is the numerical grid size and the value $s = l$ is the value of s at which the conditions of zero function and derivative at infinity are imposed as an approximation. For a given aspect ratio a, l must be taken sufficiently large to ensure no significant change in the solution. The coefficients in (17) are

$$\alpha_n = 6 + \frac{2h^2}{s_n^{\frac{1}{4}}} - \frac{2ih^4}{as_n^{\frac{1}{2}}}, \quad b_n = -4 - \frac{h^2}{s_n^{\frac{1}{4}}} + \frac{h^3}{8s_n^{\frac{5}{4}}}, \quad c_n = -4 - \frac{h^2}{s_n^{\frac{1}{4}}} - \frac{h^3}{8s_n^{\frac{5}{4}}}.$$

The solution was then obtained as follows. Arbitrary complex values were guessed for a_0 and a_1, say $a_0^{(j)}$ and $a_1^{(j)}$, and the system (16) integrated in the direction of increasing x from $x = 0$ to $x = 1$ using a fourth-order Runge–Kutta scheme. Various grid sizes in this range were used as a check on the accuracy and the step length in x typically ranged from 0·01 to 0·0025. This produced values of f, f', f'' and f''' at $s = 1$, say $f_{Ij}, f'_{Ij}, f''_{Ij}$ and f'''_{Ij} respectively. At $s = 1$ continuity of df/ds is required and in terms of the numerical scheme in the outer regime was represented by a finite-difference formula

$$(\Delta + \tfrac{1}{2}\Delta^2 - \tfrac{1}{6}\Delta^3 + \tfrac{1}{12}\Delta^4 - \tfrac{1}{20}\Delta^5) f_{-1} \approx h f'_{Ij}. \tag{18}$$

Here Δ is the forward difference operator. Since $f_0 = f_{Ij}, f_{-1}$ and f_0 may then be eliminated from the difference equations at $s = s_1$ and s_2. At the outer boundary $s = l$, $f_{n_0+2} = 0$ and f_{n_0+1} was eliminated by using a finite-difference condition similar to (18) which expresses the fact that $f'(s)$ vanishes at $s = l$. An elimination method was then used to solve the finite-difference equations. Once this had been done, sloping difference formulae, which have a truncation error $O(h^6)$ associated

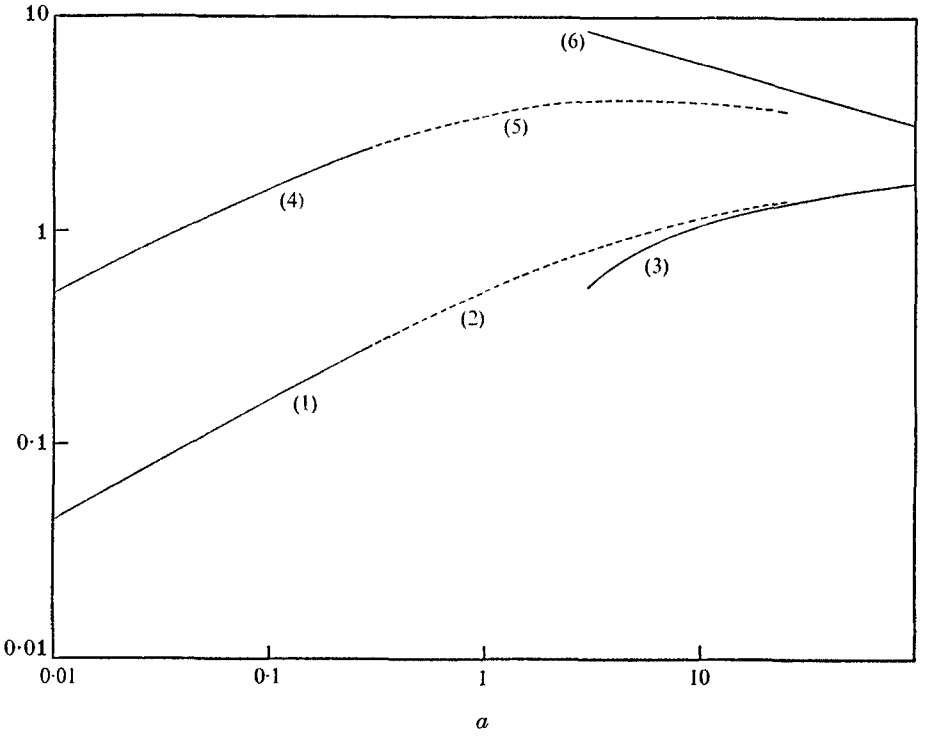

FIGURE 2. Re$\{f(0)\}$ from (1) small-a expansion, (2) numerical computation, (3) large-a expansion; Im$\{f(0)\} \times 10$ from (4) small-a expansion, (5) numerical computation, (6) large-a expansion.

with them, were used to obtain values of d^2f/ds^2 and d^3f/ds^3 at $s = 1$, say f''_{0j} and f'''_{0j}. This process was repeated with three different pairs of values $a_0^{(j)}$ and $a_1^{(j)}$. The true solution which has f and its first three derivatives continuous at $s = 1$ has

$$a_0 = \sum_{j=1}^{3} d_j a_0^{(j)}, \quad a_1 = \sum_{j=1}^{3} d_j a_1^{(j)},$$

where d_1, d_2 and d_3 are the solutions of the linear equations

$$\sum_{j=1}^{3} d_j = 1, \quad \sum_{j=1}^{3} d_j(f''_{1j} - f''_{0j}) = 0, \quad \sum_{j=1}^{3} d_j(f'''_{1j} - f'''_{0j}) = 0.$$

Having determined the correct values of a_0 and a_1, the process was repeated a fourth time to obtain the true solution.

Both the real and imaginary parts of $f(0)$ and $f'(0)$ were found to be positive and negative respectively for all values of a. The function itself is such that both real and imaginary parts oscillate about zero as s increases to infinity. It may be inferred from the asymptotic form of $f(s)$ for large s that an increasing value of a will require an increased value of l, corresponding to a larger relative width of the $E^{\frac{2}{7}}$ layer. This is because the real part of one of the appropriate roots of (10) is becoming small as a becomes large. At the largest value of a considered ($a = 25$) l was eventually taken equal to 160. As a decreases, l may be decreased but the

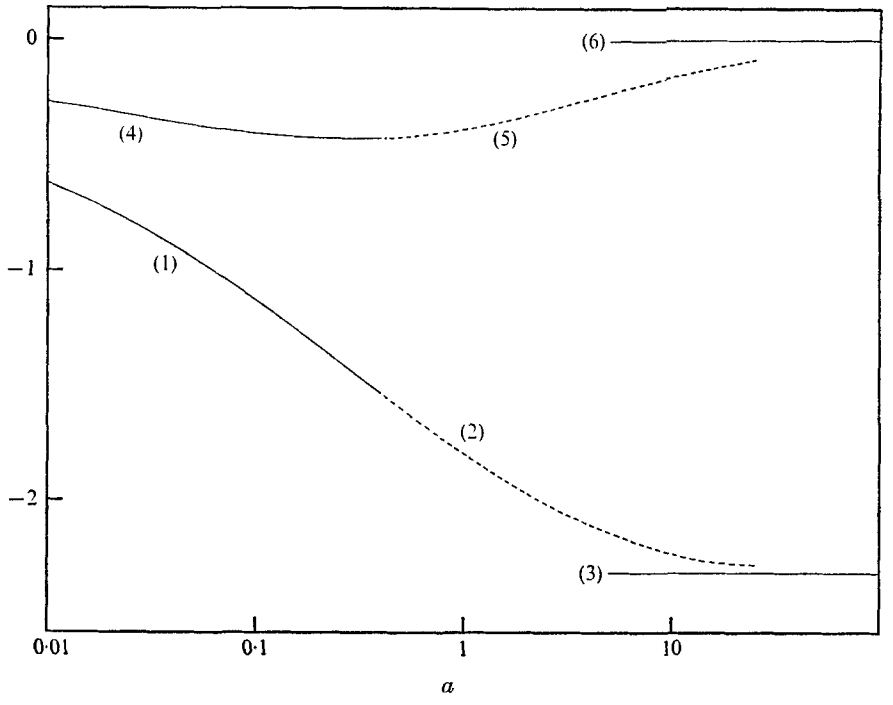

FIGURE 3. Re $\{f'(0)\}$ from (1) small-a expansion, (2) numerical computation, (3) large-a expansion; Im $\{f'(0)\}$ from (4) small-a expansion, (5) numerical computation, (6) large-a expansion.

grid size h must also be decreased accordingly. As a check on the accuracy a number of grid sizes were used for each value of a. The calculated values of $a_0 = f(0)$ and $a_1 = f'(0)$ for a in the range $[0{\cdot}01, 25]$ are plotted in figures 2 and 3 respectively. These figures also display values of these quantities calculated from the expansions of (9) for small and large a which are described in the following sections.

2.5. *Expansion for small a*

As a becomes small, the relative width of the $E^{\frac{2}{7}}$ layer shrinks; for small a set

$$t = a^{-\frac{2}{7}}s, \quad F(t) = a^{-\frac{4}{7}}f(s),$$

whereupon

$$\frac{d^4F}{dt^4} - \frac{2iF}{t^{\frac{1}{2}}} - a^{\frac{1}{2}}\frac{d}{dt}\left\{\frac{1}{t^{\frac{1}{2}}}\frac{dF}{dt}\right\} = 0,$$

and $F(t)$ may be expanded as

$$F(t) = \sum_{j=0}^{\infty} a^{\frac{1}{2}j}F_j(t).$$

The boundary conditions are

$$F_j(\infty) = \frac{dF_j}{dt}(\infty) = 0, \quad \frac{d^2F_j}{dt^2}(0) = 2^{\frac{3}{2}}\delta_{j0},$$

$$\lim_{t\to 0}\left\{\frac{d^3F_j}{dt^3} - \frac{1}{t^{\frac{1}{2}}}\frac{dF_{j-1}}{dt}\right\} = 0, \quad j \neq 0, \quad \frac{d^3F_0}{dt^3}(0) = 0,$$

j	Re $\{F_j(0)\}$	Im $\{F_j(0)\}$	Re $\{F_j'(0)\}$	Im $\{F_j'(0)\}$
0	0·6154	0·7717	−2·3502	−1·1318
1	0·0759	−0·6734	0·4682	1·3382
2	−0·3586	0·2859	0·4019	−0·8344
3	0·3080	0·0347	−0·5855	0·2048
4	−0·1306	−0·1638	0·3766	0·1814

TABLE 1. Small-a expansion: calculated values of $F_j(0)$ and $F_j'(0)$.

where δ_{j0} is the Kronecker delta. The method of numerical solution for this system is easily inferred from the preceding discussion of the solution of (9). The first nine terms of this series were calculated and the values of $F_j(0)$ and $dF_j(0)/dt$ are given in table 1 for $j = 0, \ldots, 4$. These values are sufficient to calculate values of $f(0)$ and $f'(0)$ to at least three significant figures up to $a = 0{\cdot}1$. The field length l on which the conditions at infinity were imposed was eventually taken as $l = 80$. A number of grid sizes were used in the outer region as a check on the accuracy (the smallest being $h = 0{\cdot}024$) and the results in table 1 are thought to be correct to the figures quoted. The calculated values of $f(0)$ and $f'(0)$ from the first nine terms of the expansion are plotted as solid lines in figures 2 and 3 and for $a \leqslant 0{\cdot}4$ these values were virtually identical with those calculated from the direct solution of (9) described in the preceding section.

2.6. *Expansion for large a*

The case of a large corresponds to the physical situation where the hemisphere radius is large with respect to the separation distance of the plates and for $a > 1$ the upper part of the hemisphere is sliced off by the top plate. Integrating (9) once, we obtain

$$f''' - \frac{f'}{s^{\frac{1}{4}}} = \frac{2i}{a}\int_0^s \frac{f(x)}{x^{\frac{1}{2}}}\,dx,$$

and for a large, expand

$$f(s) = f_0(s) + ia^{-1}f_1(s) + O(a^{-2}).$$

The solution for f_0 is

$$f_0(s) = \alpha_0 + \frac{2^{\frac{5}{2}}}{\Gamma(\frac{3}{7})}\left(\frac{4}{7}\right)^{\frac{3}{7}}\int_s^\infty x^{\frac{1}{2}}K_{\frac{4}{7}}(\tfrac{8}{7}x^{\frac{7}{8}})\,dx,$$

where $K_{\frac{4}{7}}$ is the Bessel function of imaginary argument and α_0 is an arbitrary constant. For s large,

$$\int_0^s \frac{f_0(x)}{x^{\frac{1}{2}}}\,dx \sim 2\alpha_0 s^{\frac{1}{2}} + \gamma_0,$$

where $\gamma_0 = 3 \times 2^{\frac{1}{2}}\,\Gamma(\frac{6}{7})\,2^{\frac{2}{7}}7^{-\frac{1}{7}}$, and therefore for s large

$$f_1 \sim \alpha_1 - \tfrac{8}{5}\gamma_0 s^{\frac{5}{4}} - \tfrac{16}{7}\alpha_0 s^{\frac{7}{4}},$$

where α_1 is an arbitrary constant. Hence

$$f(s) \sim \alpha_0\left\{1 - \frac{16i}{7a}s^{\frac{7}{4}}\right\} - \frac{8i\gamma_0}{5a}s^{\frac{5}{4}} + \frac{i\alpha_1}{a} + \ldots, \quad s \gg 1. \tag{19}$$

The functions f_0 and f_1 are the leading terms in an inner expansion which must be matched to an outer expansion. If we define outer variables

$$z = a^{-\frac{4}{7}}s, \quad \tilde{F}(z) = f(s),$$

then $\tilde{F}$ satisfies

$$\frac{d^2\tilde{F}}{dz^2} - \frac{1}{4z}\frac{d\tilde{F}}{dz} + \frac{2i\tilde{F}}{z^{\frac{1}{4}}} = \frac{z^{\frac{1}{4}}}{a}\frac{d^4\tilde{F}}{dz^4},$$

and $\tilde{F}$ is expanded as

$$\tilde{F}(z) = \tilde{F}_0(z) + a^{-1}\tilde{F}_1(z) + O(a^{-2}).$$

The solution for $\tilde{F}_0(z)$ which vanishes as $z \to \infty$ and for which $\tilde{F}_0(0) = \alpha_0$ is

$$\tilde{F}_0(z) = \frac{2\alpha_0}{\Gamma(\frac{5}{7})} c_0^{\frac{5}{7}} z^{\frac{5}{8}} K_{\frac{5}{7}}(2c_0 z^{\frac{7}{8}}),$$

where $c_0 = 8e^{-\frac{1}{4}i\pi}/7 \times 2^{\frac{1}{2}}$. Setting $s = a^{\frac{4}{7}}z$ in (19) we require that $\tilde{F}(z)$ as $z \to 0$ match $f(s)$ for large s. A match of the $z^{\frac{5}{4}}$ term in both expressions fixes α_0 as

$$\alpha_0 = 3i\left(\frac{7}{a}\right)^{\frac{2}{7}} 2^{\frac{3}{14}} \frac{\Gamma(\frac{5}{7})\,\Gamma(\frac{6}{7})}{\Gamma(\frac{2}{7})} e^{-\frac{5}{14}\pi i}.$$

In figure 2 the leading term from the large-a expansion is plotted as

$$f(0) \approx \alpha_0 + 2^{\frac{1}{7}}7^{\frac{2}{7}}2^{\frac{3}{7}}\,\Gamma(\tfrac{8}{7})\,\Gamma(\tfrac{4}{7})/\Gamma(\tfrac{3}{7}). \tag{20}$$

In figure 3, the leading term for $f'(0)$ for large a is given as

$$f'(0) \approx -2^{\frac{3}{2}}(\tfrac{7}{4})^{\frac{1}{7}}\,\Gamma(\tfrac{4}{7})/\Gamma(\tfrac{3}{7}). \tag{21}$$

The leading error term in both (20) and (21) is $O(a^{-1})$ and the calculated values of $f(0)$ and $f'(0)$ are clearly approaching expressions (20) and (21) for a large.

2.7. *Continuation of the expansion in the outer layers*

Suppose that, for a given aspect ratio a, the solution in the $E^{\frac{5}{7}}$ layer has been determined to leading order, so that $a_0 = f(0)$ and $a_1 = f'(0)$ are known. In general a_0 and a_1 are non-zero complex constants, which implies a non-zero swirl and radial velocity $O(E^{\frac{1}{28}})$ and $O(E^{\frac{9}{28}})$ respectively at $r = a-$. Since continuity of u and v across the $E^{\frac{1}{3}}$ layer is required, the expansion is continued in the outer layers as follows: in the $E^{\frac{1}{4}}$ layer,

$$v_{\frac{1}{4}} = v_0(\xi,\theta) + \left(\frac{2}{a}\right)^{\frac{1}{7}} E^{\frac{1}{28}} v_1(\xi,\theta) + \left(\frac{2}{a}\right)^{\frac{2}{7}} E^{\frac{1}{14}} v_2(\xi,\theta) + \ldots,$$

$$u_{\frac{1}{4}} = \frac{E^{\frac{1}{4}}}{2^{\frac{1}{2}}a}\left\{u_0(\xi,\theta) + \left(\frac{2}{a}\right)^{\frac{1}{7}} E^{\frac{1}{28}} u_1(\xi,\theta) + \left(\frac{2}{a}\right)^{\frac{2}{7}} E^{\frac{1}{14}} u_2(\xi,\theta) + \ldots\right\},$$

and in the $E^{\frac{2}{7}}$ layer

$$v_{\frac{2}{7}} = \left(\frac{2}{a}\right)^{\frac{1}{7}} E^{\frac{1}{28}}\left\{\bar{v}_0(s,\theta) + \left(\frac{2}{a}\right)^{\frac{1}{7}} E^{\frac{1}{28}} \bar{v}_1(s,\theta) + \left(\frac{2}{a}\right)^{\frac{2}{7}} E^{\frac{1}{14}} \bar{v}_2(s,\theta) + \ldots\right\},$$

$$u_{\frac{2}{7}} = \frac{1}{a}\left(\frac{2}{a}\right)^{\frac{2}{7}} E^{\frac{9}{28}}\left\{\bar{u}_0(s,\theta) + \left(\frac{2}{a}\right)^{\frac{1}{7}} E^{\frac{1}{28}} \bar{u}_1(s,\theta) + \left(\frac{2}{a}\right)^{\frac{2}{7}} E^{\frac{1}{14}} \bar{u}_2(s,\theta) + \ldots\right\}.$$

The solution for u_1 and v_1 is

$$v_1 = \mathrm{Re}\,(-ia_1 e^{-\xi+i\theta}), \quad u_1 = \mathrm{Re}\,(a_1 e^{i\theta}(e^{-\xi}-1)),$$

where u_1 vanishes at $\xi = 0$ since the lowest-order term in u in the $E^{\frac{2}{7}}$ layer is $O(E^{\frac{9}{28}})$. Thus the leading-order flow in the $E^{\frac{2}{7}}$ layer, which is not symmetrical about $\theta = 0, \pi$, has generated asymmetrical velocities in the $E^{\frac{1}{4}}$ layer. The equations for $\bar{v}_1$ and $\bar{u}_1$ are identical to those for $\bar{v}_0$ and $\bar{u}_0$. Setting

$$\bar{v}_1 = \mathrm{Re}\,(-if_1'(s)\,e^{i\theta}), \quad \bar{u}_1 = \mathrm{Re}\,(f_1(s)\,e^{i\theta}),$$

where $f_1(s)$ satisfies the same equation (9) as $f(s)$, then continuity of $\partial v/\partial r$ across the $E^{\frac{1}{3}}$ layer and the flux condition (11) respectively lead to the two conditions

$$f_1''(0) = 2^{\frac{1}{2}}a_1, \quad \lim_{s\to 0}\{f_1''' - f_1'/s^{\frac{1}{4}}\} = 4.$$

In principle, $f_1(s)$ may be obtained numerically, yielding a value $f_1'(0) = a_{11}$, say, and the solution for u_2 and v_2 is then

$$v_2(\xi,\theta) = \mathrm{Re}\{-ia_{11}e^{-\xi+i\theta}\},$$
$$u_2(\xi,\theta) = \mathrm{Re}\{2^{\frac{1}{2}}a_0 e^{i\theta} + a_{11}e^{i\theta}(e^{-\xi}-1)\}.$$

Higher-order terms in the expansion can be calculated, although from this stage onwards neglected terms in the Ekman conditions in the $E^{\frac{2}{7}}$ layer enter the equations and at a later stage in the $E^{\frac{1}{4}}$ layer. We do not pursue this further since the only point of interest here is that all velocities with the exception of the leading term in the $E^{\frac{1}{4}}$ layer are asymmetric about $\theta = 0, \pi$. The consequences of this in connexion with the geostrophic flow for $r > a$ will be examined subsequently.

In the $E^{\frac{1}{3}}$ layer, the velocity components are written as

$$\left.\begin{aligned}
v_{\frac{1}{3}} &= \mathrm{Re}\left[\left\{\left(\frac{2}{a}\right)^{\frac{1}{7}} E^{\frac{1}{28}}a_1 - 2^{\frac{3}{2}}\eta E^{\frac{1}{12}} + E^{\frac{5}{42}}\tilde{v}_1 + E^{\frac{13}{84}}\tilde{v}_2 + \ldots\right\}\{-i\,e^{i\theta}\}\right],\\
w_{\frac{1}{3}} &= \mathrm{Re}\,[\{E^{\frac{5}{42}}\tilde{w}_1 + E^{\frac{13}{84}}\tilde{w}_2 + \ldots\}\{-i\,e^{i\theta}\}],\\
u_{\frac{1}{3}} &= \mathrm{Re}\left[\left\{\frac{1}{a}\left(\frac{2}{a}\right)^{\frac{2}{7}} a_0 E^{\frac{9}{28}} - \frac{1}{a}\left(\frac{2}{a}\right)^{\frac{1}{7}} a_1 E^{\frac{31}{84}}\eta + \frac{2^{\frac{1}{2}}}{a}E^{\frac{35}{84}}\eta^2 + E^{\frac{10}{42}}\tilde{u}_1 + E^{\frac{41}{84}}\tilde{u}_2 + \ldots\right\}e^{i\theta}\right].
\end{aligned}\right\} \tag{22}$$

The solutions for the leading terms $\tilde{v}_1$ and $\tilde{w}_1$ are essentially those given by Stewartson (1966).

2.8. *The flow in the $E^{\frac{2}{7}}$ layer*

One point of interest regarding the shear layers concerns the particle paths in the $E^{\frac{2}{7}}$ layer. A stream function $\psi(r,\theta)$ is defined by

$$v = \frac{\partial\psi}{\partial r}, \quad u = -\frac{1}{r}\frac{\partial\psi}{\partial\theta}, \quad \psi(a-,\theta) = 0.$$

Here ψ is defined as zero in the stagnant region above the hemisphere. The stream function in the $E^{\frac{2}{7}}$ layer is

$$\psi(s,\theta) = \left(\frac{2}{a}\right)^{\frac{1}{7}} E^{\frac{2}{7}}\int_s^\infty v_{\frac{2}{7}}\,ds,$$

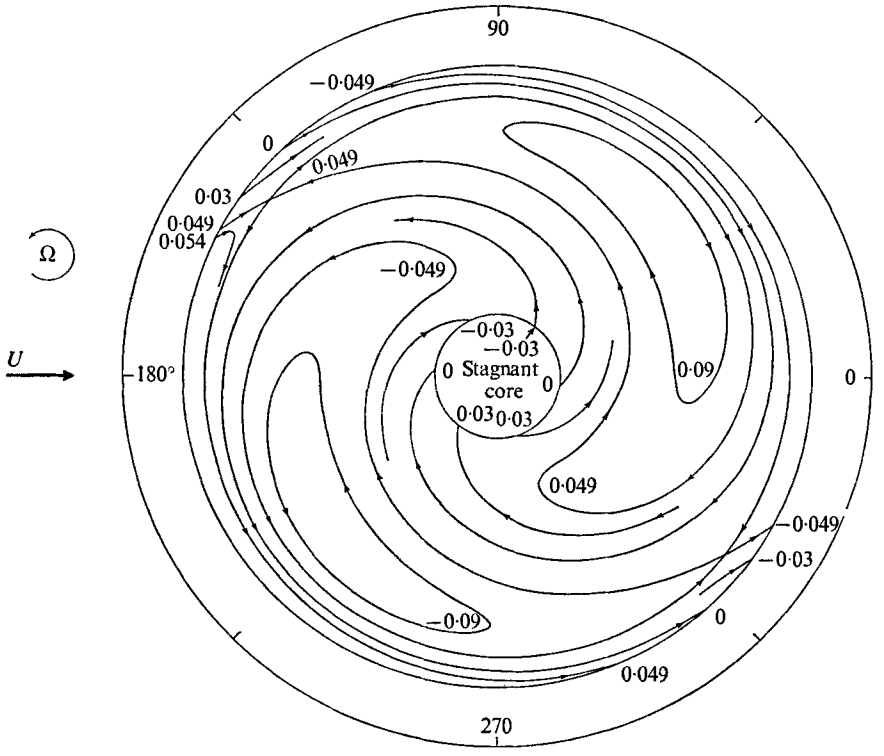

FIGURE 4. Projections of streamlines in the $E^{\frac{2}{7}}$ layer (not to scale).

and to leading order

$$\psi = (2/a)^{\frac{2}{7}} E^{\frac{9}{28}} \overline{\psi} + O(E^{\frac{5}{14}}), \quad \overline{\psi} = \mathrm{Re}\{if(s)\, e^{i\theta}\}.$$

In figure 4 the lines of constant $\overline{\psi}$ are plotted for the case $a = 0{\cdot}05$. This picture represents the projections of streamlines that an observer looking down from above would see. Here the region of the thin $E^{\frac{2}{7}}$ layer has been blown up out of scale for closer inspection. The outer circle corresponds to the hemisphere rim while the inner circle corresponds to the edge of the stagnant interior. For the case $a = 0{\cdot}05$ the boundary on which the zero conditions for $f(s)$ were imposed was taken at $l = 26$ but in figure 4 only the region between $s = 0$ and $s = 2$ is plotted. All the salient features of the flow can be inferred from figure 4 though.

The flow is separated into two antisymmetrical parts by the two spiral arms of the line $\overline{\psi} = 0$ A particle which crosses the rim from upstream on this line will spiral in towards the stagnant interior, progressively slowing down as it penetrates deeper. Conversely on the other line $\overline{\psi} = 0$ particles are accelerated from the stagnant interior, spiral out and eventually leave downstream as they cross the rim in the fourth quadrant. It is only on these paths that a particle can either penetrate or leave the stagnant interior. Both however are limiting projected streamlines and envelopes of the other path lines. As such there is zero actual transfer of fluid from the stagnant interior.

Since the flow for lines of negative $\overline{\psi}$ is the reflexion of that for positive $\overline{\psi}$ except that the direction of the velocity vector is reversed we need only discuss the flow for lines of positive $\overline{\psi}$. The projected streamline labelled 0·03 is similar to the type of particle path that is the basis of the motion in Jacobs' (1964) solution for a lenticular body. A particle on this path crosses the rim in the second quadrant and spirals down between the lines $\overline{\psi} = 0$ and $\overline{\psi} = 0{\cdot}049$. (To avoid overcrowding in figure 4, the entire line $\overline{\psi} = 0{\cdot}03$ has not been drawn in.) The path $\overline{\psi} = 0{\cdot}03$ is shown terminating in the third quadrant at the stagnant interior but this is only because of a space limitation in the diagram. A particle on this path continues to spiral inward until eventually it reverses direction and spirals back out to the rim. The path $\overline{\psi} = 0{\cdot}03$ is shown emerging again in the fourth quadrant whereupon it circles around and eventually passes out over the rim in the fourth quadrant. All particles on path lines between $\overline{\psi} = 0$ and $\overline{\psi} = 0{\cdot}049$ will move in this reversing spiral motion.

The interesting difference between the hemisphere and the lenticular body (Jacobs 1964) is the appearance of two trapped eddies in the inner layer of which the projected streamline $\overline{\psi} = 0{\cdot}049$ is approximately the limiting path line. Within this line, particles appear to be forced to recirculate (e.g. $\overline{\psi} = 0{\cdot}09$). In general there are four stagnation points: (*a*) at the centre of the eddies in the first and third quadrants and (*b*) at the edge of the limiting projected streamlines $\overline{\psi} = 0{\cdot}049$ in the second and fourth quadrants. The condition for a stagnation point is $u = v = 0$ or

$$\mathrm{Re}\,(f(s)\,e^{i\theta}) = \mathrm{Re}\,(if'(s)\,e^{i\theta}) = 0,$$

and eliminating θ from these equations gives

$$\mathrm{Re}\{f'(s)f^*(s)\} = 0 \quad \text{or} \quad d|f|^2/ds = 0.$$

This is not an unreasonable condition and was found to be satisfied by $f(s)$ for all numerical solutions at two points in the range of s. Outside the eddy, particles on the line $\overline{\psi} = 0{\cdot}049$ cross the rim in the second quadrant, are subsequently turned away from the stagnation point and circle around, passing over the rim in the fourth quadrant.

The appearance of the trapped eddies appears at first sight disturbing. This is because associated with this motion there is a weak vertical motion [$O(E^{\frac{5}{28}})$]. This vertical velocity is continually changing sign in the $E^{\frac{2}{7}}$ layer and, for example, part of the projected streamline $\overline{\psi} = 0{\cdot}09$ lies in a region of positive vertical velocity and part in a region of negative vertical velocity. However some closed path lines near the eddy centre in the second quadrant lie entirely in a region of positive vertical velocity. Since the Ekman condition at the top plate requires zero vertical velocity there, this appears to be of some concern since to leading order there can be no net transfer of fluid to the top Ekman layer. We first remark that the time required for a particle to complete a closed circuit is $O(E^{-\frac{1}{28}})$ while the time required for it to travel an $O(1)$ distance in the vertical direction is $O(E^{-\frac{5}{28}})$. The fluid particles must therefore traverse an infinite number of circuits before moving an $O(1)$ distance away from or towards the top Ekman layer.

Whether or not these trapped eddies are an actual feature of the flow is not known. One possibility is that what to leading order appears as a two-dimensional

closed-circuit motion may in reality be found to be a spiral motion to (or away from) a point when the higher-order terms are considered. Consider for example the motion

$$U = y, \quad V = -x, \quad W = 0,$$

where (x, y, z) are rectangular Cartesian co-ordinates and (U, V, W) are the corresponding velocity components. This is a two-dimensional motion wherein the streamlines are concentric circles centred at $x = y = 0$. If we now consider a perturbation to this motion

$$U = y - \delta x, \quad V = -x, \quad W = \delta(z-1),$$

where δ is a small constant, then a projection of the particle paths in a plane of constant z indicates that the particles spiral slowly away from or towards $x = y = 0$ depending on the sign of δ.

Another possibility is that the higher-order terms in the expansions for $u_{\frac{2}{7}}$ and $v_{\frac{2}{7}}$ act to displace the eddies in such a way that through every closed circuit in a plane of constant z there is no net flux of fluid. To attempt to verify this would be a formidable task since this would involve the calculation of five terms in the expansions for $u_{\frac{2}{7}}$ and $v_{\frac{2}{7}}$. It is only at the stage when $v_{\frac{2}{7}}$ contains a term $O(E^{\frac{5}{28}})$ that the leading-order vertical velocity $\overline{w}_0(s, \theta, z)$ enters the continuity equation. This possibility seems the most likely but the question remains unresolved here.

2.9. *Modification of the geostrophic flow*

Lastly a complete match may now be made with the geostrophic flow for $r > a$. In the $E^{\frac{1}{4}}$ layer the stream function is

$$\psi(\xi, \theta) = \frac{E^{\frac{1}{4}}}{2^{\frac{1}{2}}} \int_0^{\xi} v_{\frac{1}{4}} d\xi + \left(\frac{2}{a}\right)^{\frac{1}{7}} E^{\frac{2}{7}} \int_0^{\infty} v_{\frac{2}{7}} ds. \tag{23}$$

For $r > a+$, to $O(E^{\frac{1}{2}})$ the geostrophic stream function is harmonic and

$$\psi_G(r, \theta) = -r \sin\theta + \sum_{n=1}^{\infty} \left\{ \frac{C_n}{r^n} \cos n\theta + \frac{D_n}{r^n} \sin n\theta \right\}. \tag{24}$$

For ξ large, $\psi(\xi, \theta)$ must match $\psi_G(r, \theta)$ as $r \to a+$ and by writing $r = a + \xi E^{\frac{1}{4}}/2^{\frac{1}{2}}$ in (24), this can be shown to be satisfied if

$$D_1 = a^2 + 2^{\frac{1}{2}} a E^{\frac{1}{4}} + (2/a)^{\frac{1}{7}} 2^{-\frac{1}{2}} a E^{\frac{2}{7}} \operatorname{Re}(a_1) + O(E^{\frac{9}{28}}),$$

$$C_1 = (2/a)^{\frac{1}{7}} 2^{-\frac{1}{2}} a E^{\frac{2}{7}} \operatorname{Im}(a_1) + O(E^{\frac{9}{28}}),$$

$$D_n = C_n = 0, \quad n > 1.$$

Thus for $r > a$

$$V_G = -\sin\theta \left(1 + \frac{D_1}{r^2}\right) - \frac{C_1}{r^2} \cos\theta, \quad U_G = \cos\theta \left(1 - \frac{D_1}{r^2}\right) + \frac{C_1}{r^2} \sin\theta \tag{25}$$

and a weak asymmetric flow $[O(E^{\frac{2}{7}})]$ about $\theta = 0, \pi$ is present. In order to make a qualitative comparison with Baker's photograph (Greenspan 1968, p. 3) and the photographs of Hide *et al.* (1968) it is necessary to know what the sign of C_1 is in general. If the procedure of the latter part of § 2.3 is repeated using the correct boundary conditions (15) for $f(s)$ rather than (14), it may be shown that

$$2^{\frac{3}{2}} f'(0) = -\int_0^{\infty} \left\{ |f''|^2 + \frac{|f'|^2}{s^{\frac{1}{4}}} + \frac{2i\,|f|^2}{a s^{\frac{1}{2}}} \right\} ds.$$

Therefore for all a, $a_1 = f'(0)$ has negative real and imaginary parts and since C_1 is negative for all a, the asymmetric terms in (25) yield weak velocities which will tend to produce the experimentally observed asymmetry.

3. Nonlinear theory

To investigate the nonlinear modifications to the flow when $\epsilon \neq 0$ we consider the case when $\epsilon = O(E^{\frac{1}{2}})$. For a Rossby number of this order of magnitude the inertial terms in the swirl momentum equation become of the same order of magnitude as the viscous stress in the $E^{\frac{1}{4}}$ layer. Barcilon (1970) has shown that, provided $\epsilon \ll 1$, inertial effects in the Ekman layers, which control an $O(1)$ geostrophic flow, may be neglected and hence the linear Ekman conditions may still be used in the present case. Setting

$$\epsilon = a\lambda E^{\frac{1}{2}},$$

where λ is an $O(1)$ constant, the zeroth-order equation for the geostrophic flow for $r > a$ may be obtained as

$$a\lambda\left\{U_G\frac{\partial\zeta_G}{\partial r}+\frac{V_G}{r}\frac{\partial\zeta_G}{\partial\theta}\right\}+2\zeta_G = 0+O(E^{\frac{1}{2}}).$$

Therefore to lowest order the two-dimensional irrotational solution (4) is still appropriate in the nonlinear case for $r > a$. For $r < a$, the Ekman condition (3) gives $U_G = 0$ and it may be readily shown that any axially symmetric solution must be stagnant over the hemisphere.

In the shear layers the same expansion for the velocity components and pressure is used as in the linear theory. According to the expansion (7) it may be easily verified that nonlinear effects do not become important in the $E^{\frac{2}{7}}$ layer until $\epsilon = O(E^{\frac{11}{28}})$. Bearing in mind that the form of the solution in the $E^{\frac{1}{3}}$ layer will be analogous to (22) it may be deduced that nonlinear effects in the $E^{\frac{1}{3}}$ layer become important when $\epsilon = O(E^{\frac{29}{84}})$. In the Ekman layers which bracket the $E^{\frac{2}{7}}$ and $E^{\frac{1}{4}}$ layers and also the $E^{\frac{1}{3}}$ layer, nonlinear effects are important when $\epsilon = O(E^{\frac{1}{4}})$ and $O(E^{\frac{25}{84}})$ respectively. In the boundary-layer context all of these orders of magnitude are much greater than $O(E^{\frac{1}{2}})$ and hence these layers may be treated as being linear. Because at this stage nonlinear effects are only important in the $E^{\frac{1}{4}}$ layer, the arguments that led to

$$u_0(\xi,\theta) = v_0(\xi,\theta) = 0 \quad \text{at} \quad \xi = 0 \tag{26}$$

in the linear case are still valid. Thus the leading-order motion in the nonlinear $E^{\frac{1}{4}}$ layer is identical to that for flow past a solid circular cylinder in a rotating frame. In a recent paper, Walker & Stewartson (1972) in their study of this latter problem derived the equations satisfied by u_0 and v_0 when $\epsilon = O(E^{\frac{1}{2}})$ and the result is simply quoted here. If $N = 2/\lambda$ then

$$u_0\frac{\partial v_0}{\partial\xi}+v_0\frac{\partial v_0}{\partial\theta} = V_G\frac{\partial V_G}{\partial\theta}+N(V_G-v_0)+N\frac{\partial^2 v_0}{\partial\xi^2}, \tag{27}$$

with

$$u_0 = -\int_0^\xi \frac{\partial v_0}{\partial\theta}\,d\xi. \tag{28}$$

Here the geostrophic velocity V_G in (27) is evaluated at $r = a+$. The boundary conditions for this system are (26) and

$$v_0(\xi, \theta) \to -2\sin\theta = V_G(a+, \theta) \quad \text{as} \quad \xi \to \infty.$$

The terms neglected in deriving these equations are $O(E^{\frac{1}{4}})$. Equations (27) and (28) arise in the study of the viscous boundary layer on a cylinder with an associated applied radial magnetic field which is strong in the sense that induced fields may be neglected. There the parameter N is termed the interaction parameter and is the square of the Hartmann number divided by the Reynolds number. This problem has been studied by Leibovich (1967) and Buckmaster (1969, 1971).

Leibovich (1967) considered the flow in the vicinity of the rear stagnation point of the cylinder and showed that a similarity solution of the form $u_0 = \theta f'(\xi)$ could be found if and only if $N > 4$. (Leibovich's (1967) analysis was for a general bluff body and his interaction parameter is based on the local inviscid velocity gradient at the rear stagnation point.) Thus for $N > 4$ ($\epsilon < \frac{1}{2}aE^{\frac{1}{2}}$), separation does not occur and the flow in the $E^{\frac{1}{4}}$ layer is completely attached around the perimeter of the Taylor column.

For $2 < N < 4$, Leibovich (1967) suggested that separation without reversed flow would occur and that the flow was inherently unsteady. The meaning of the former conclusion is unclear and was disputed by Buckmaster (1969), who argued that separation would not occur in this range of N. He presented a number of arguments to substantiate this including a numerical integration of the boundary-layer equations. In a subsequent paper, Buckmaster (1971) examined this range of N in more detail and concluded that the flow in an inviscid region of the boundary layer at large distances from the body is unsteady. In the present problem this suggests a possible unsteadiness in the outer regions of the $E^{\frac{1}{4}}$ layer but no separation when $\frac{1}{2}aE^{\frac{1}{2}} < \epsilon < aE^{\frac{1}{2}}$.

For $N < 2$, Leibovich (1967), using methods similar to those of Proudman & Johnson (1962), showed that the flow in the vicinity of the rear stagnation point was inherently unsteady with a growing inviscid region dominated by eddies. The flow near the back of the cylinder is ultimately ($t \to \infty$) that for a forward stagnation point. In the present context then, if $\epsilon > aE^{\frac{1}{2}}$ separation takes place in the $E^{\frac{1}{4}}$ layer; the interesting difference here is that, unlike the case of a solid cylinder, separation occurs at a fluid–fluid interface in a free shear layer. We remark here that, while the theory asserts that no steady solution exists for $\epsilon > aE^{\frac{1}{2}}$ and that separation takes place, it does not discuss the subsequent time-dependent development of the separated region. The prime result here is that the free shear layer breaks down at separation, a consequence which could not possibly be predicted from the basic linear theory. This conclusion is supported by experiments where there is observed to be a breakaway of the free shear layer which looks remarkably like the classical separation.

4. Concluding remarks

It is now a relatively simple exercise to consider the Taylor-column problem for flow past a general symmetrical obstacle which has an infinite slope at the rim ($r = a$). Let the obstacle be such that

$$z \to C(a-r)^n \quad \text{as} \quad r \to a, \quad \text{where} \quad 0 < n < 1.$$

The leading terms for the expansions of the velocity components are the same in the external $E^{\frac{1}{4}}$ layer as in the hemisphere case but the width of the $E^{\frac{2}{7}}$ layer is now modified to $O(E^{\beta})$, where $\beta = 1/(n+3)$. In this layer, the leading terms for the velocity components are

$$u_\beta = a^{-1}(nC)^{-2\beta} E^{\frac{1}{4}(5-n)\beta} \tilde{u}(x,\theta) + \ldots,$$
$$v_\beta = (nC)^{-\beta} E^{\frac{1}{4}(1-n)\beta} \tilde{v}(x,\theta) + \ldots,$$
$$w_\beta = (nC)^{2\beta} E^{\frac{1}{4}(3n+1)\beta} \tilde{w}(x,\theta,z) + \ldots,$$

where $x = (nC)^{\beta}(a-r)\,E^{-\beta}$ is the scaled radial variable in the E^{β} layer. The functions $\tilde{u}$, $\tilde{v}$ and $\tilde{w}$ are $O(1)$ functions of (x,θ) and it may be shown that

$$\frac{\partial^2 \tilde{v}}{\partial x^3} - \frac{\partial}{\partial x}\left\{\frac{\tilde{v}}{x^{\frac{1}{2}(1-n)}}\right\} - \frac{2\tilde{u}}{ax^{1-n}} = 0, \quad \frac{\partial \tilde{u}}{\partial x} = \frac{\partial \tilde{v}}{\partial \theta}.$$

This system with an appropriate flux condition and continuity of v and $\partial v/\partial r$ across the $E^{\frac{1}{4}}$ layer can in principle be solved in an analogous manner to the method of solution for the leading term in the $E^{\frac{2}{7}}$ layer for the hemisphere. In particular, the arguments that led to the zero boundary conditions (26) for the components u_0 and v_0 in the external $E^{\frac{1}{4}}$ layer may be repeated. The implication of this is that, in the nonlinear case, separation also occurs in the external $E^{\frac{1}{4}}$ layer for these obstacles when $\epsilon > aE^{\frac{1}{2}}$.

One further point is of interest in this connexion. As n becomes small the width of the E^{β} layer becomes arbitrarily close to $O(E^{\frac{1}{3}})$ and the leading terms for v_β and w_β become of the same magnitude $[O(E^{\frac{1}{12}})]$. This is in accordance with the work of Foster (1972), who considered the linear theory for flow past a circular cylindrical obstacle. He found that while there is an external $E^{\frac{1}{4}}$ layer at $r = a+$, there is only an internal $E^{\frac{1}{3}}$ layer above the cylinder.

Finally the separation criterion ($\epsilon > aE^{\frac{1}{2}}$) can also be shown to be appropriate in the case of an arbitrary spheroid translating in a straight line transversely to the rotation axis in a contained rapidly rotating fluid. In this case, the work of Moore & Saffman (1969*a*, *b*) shows that the correct matching conditions are continuity of swirl velocity and total tangential stress (not local) across the $E^{\frac{1}{3}}$ layer. In this case the boundary conditions (26) for the functions u_0 and v_0 in the external $E^{\frac{1}{4}}$ layer can again be deduced.

The authors are grateful for a number of stimulating discussions with Prof. R. Hide, Dr L. M. Hocking and Prof. W. P. Graebel. Part of this work was supported by a grant from the National Research Council of Canada.

REFERENCES

BARCILON, V. 1970 Some inertial modifications of the linear viscous theory of steady rotating fluid flows. *Phys. Fluids*, **13**, 537–544.

BUCKMASTER, J. 1969 Separation and magnetohydrodynamics. *J. Fluid Mech.* **38**, 481–498.

BUCKMASTER, J. 1971 Boundary layer structure at a magnetohydrodynamic rear stagnation point. *Quart. J. Mech. Appl. Math.* **24**, 373–386.

FOSTER, M. R. 1972 The flow caused by the differential rotation of a right circular cylindrical depression in one of two rapidly rotating parallel planes. *J. Fluid Mech.* **53**, 647–655.

GRACE, S. F. 1926 On the motion of a sphere in a rotating liquid. *Proc. Roy. Soc.* A **113**, 46–77.

GREENSPAN, H. 1968 *The Theory of Rotating Fluids*. Cambridge University Press.

HIDE, R. & IBBETSON, A. 1966 An experimental study of 'Taylor' columns. *Icarus*, **5**, 279–290.

HIDE, R., IBBETSON, A. & LIGHTHILL, M. J. 1968 On slow transverse flow past obstacles in a rapidly rotating fluid. *J. Fluid Mech.* **32**, 251–272.

JACOBS, S. J. 1964 The Taylor column problem. *J. Fluid Mech.* **20**, 581–591.

LEIBOVICH, S. 1967 Magnetohydrodynamic flow at a rear stagnation point. *J. Fluid Mech.* **29**, 401–413.

MOORE, D. W. & SAFFMAN, P. G. 1969*a* The structure of free vertical shear layers in a rotating fluid and the motion produced by a slowly rising body. *Phil. Trans.* A **264**, 597–634.

MOORE, D. W. & SAFFMAN, P. G. 1969*b* The flow induced by the transverse motion of a thin disk in its own plane through a contained rapidly rotating fluid. *J. Fluid Mech.* **39**, 831–847.

PROUDMAN, I. & JOHNSON, K. 1962 Boundary-layer growth near a rear stagnation point. *J. Fluid Mech.* **12**, 161–168.

STEWARTSON, K. 1953 On the slow motion of an ellipsoid in a rotating fluid. *Quart. J. Mech.* **7**, 141–162.

STEWARTSON, K. 1966 On almost rigid rotations. Part 2. *J. Fluid Mech.* **26**, 131–144.

STEWARTSON, K. 1967 On the slow transverse motion of a sphere through a rotating fluid. *J. Fluid Mech.* **30**, 357–369.

TAYLOR, G. I. 1922 The motion of a sphere in a rotating liquid. *Proc. Roy. Soc.* A **102**, 180–189.

TAYLOR, G. I. 1923 Experiments on the motion of solid bodies in rotating fluids. *Proc. Roy. Soc.* A **104**, 213–218.

WALKER, J. D. A. & STEWARTSON, K. 1972 The flow past a circular cylinder in a rotating frame. *Z. angew. Math. Phys.* **23**, 745–752.